PCCP

PAPER

Cyclohexane oxidation using Au/MgO: an investigation of the reaction mechanism

Marco Conte,*[a] Xi Liu,[a] Damien M. Murphy,[a] Keith Whiston[b] and Graham J. Hutchings*[a]

The liquid phase oxidation of cyclohexane was undertaken using Au/MgO and the reaction mechanism was investigated by means of continuous wave (CW) EPR spectroscopy employing the spin trapping technique. Activity tests aimed to determine the conversion and selectivity of Au/MgO catalyst showed that Au was capable of selectivity control to cyclohexanol formation up to 70%, but this was accompanied by a limited enhancement in conversion when compared with the reaction in the absence of catalyst. In contrast, when radical initiators were used, in combination with Au/MgO, an activity comparable to that observed in industrial processes at *ca.* 5% conversion was found, with retained high selectivity. By studying the free radical autoxidation of cyclohexane and the cyclohexyl hydroperoxide decomposition in the presence of spin traps, we show that Au nanoparticles are capable of an enhanced generation of cyclohexyl alkoxy radicals, and the role of Au is identified as a promoter of the catalytic autoxidation processes, therefore demonstrating that the reaction proceeds *via* a radical chain mechanism.

1. Introduction

The partial oxidation of cyclohexane to cyclohexanone and cyclohexanol is a major process in industrial chemistry since these two products are chemical precursors for the manufacture of nylon-6 and nylon 6,6 fibres *via* oxidation to adipic acid.[1] Typically this reaction is carried out in the liquid phase under aerobic conditions using air as oxidant at 125–160 °C and 3–15 bar, normally using cobalt-based homogeneous catalysts, such as cobalt(II)-naphthenate or cobalt acetylacetonate.[2,3] The reaction is known to proceed by a free radical autoxidation mechanism.[4,5] Heterogeneous catalysts such as MoO_3, Cr_2O_3 and WO_3 have also been reported,[6] and gas phase catalytic oxidation can be used.[7] However, the major drawback of these processes lies in the poor selectivity control to cyclohexanol and cyclohexanone. In fact, in order to avoid the formation of a high organic acid content, and to preserve a high selectivity to the alcohol and the ketone (>70%), conversion values are industrially limited to 4–12%.[8,9] This prompted several research groups to explore the possibility of developing new catalysts, for example using gold-based catalysts for the liquid phase oxidation of cyclohexane[10–14] because of the efficiency of these materials in a vast array of selective oxidation reactions.[15–17]

However, it is currently debated if gold-based materials are real catalytic systems or rather act as promoters of the autoxidation pathways for the cyclohexane oxidation reaction.[18] SiO_2 supported gold catalysts, modified by doping with TiO_2, were reported to be capable of high conversion,[19,20] relative to the industrial catalyst, of *ca.* 10% and selectivity to the alcohol and ketone (K/A oil) > 70%, which was not observed in the absence of supported gold nanoparticles; the conclusion reached was that this was a real catalyst for cyclohexane oxidation. On the other hand, investigation of the cyclohexane oxidation over Au/Al_2O_3, Au/TiO_2 and Au/SBA-15[21] showed that the reaction proceeds *via* a pure radical pathway with products typical of autoxidation and the reaction could be fully inhibited by means of radical scavengers. Finally, it has also been shown that gold nanoclusters supported on hydroxyapatite were capable of displaying high activity towards cyclohexane[22] and that no reaction was taking place in the absence of gold, although the reaction required the presence of radical initiators, typically *tert*-butylhydroperoxide (TBHP).

This lack of unambiguous evidence on the true catalytic role of gold in the cyclohexane oxidation, prompted us to carry out a mechanistic study using Au/MgO because of its excellent selective oxidation properties.[23–25] To test if the cyclohexane oxidation reaction proceeds *via* a radical mechanism, we employed X-band EPR spectroscopy combined with the spin trapping technique[26–28] as well as radical scavengers. The principle of the spin-trapping methodology relies on the fast selective addition, *i.e.* trapping, of short-lived radicals to a diamagnetic spin trap, usually a nitrone or a nitroso compound, such as 5,5-dimethyl-1-pyrroline-*N*-oxide (DMPO). The product of

[a] *Cardiff Catalysis Institute, School of Chemistry, Cardiff University, Cardiff, CF10 3AT, UK. E-mail: ConteM1@cardiff.ac.uk, Hutch@cardiff.ac.uk*
[b] *INVISTA Textiles (UK) Limited, P.O. Box 2002, Wilton, Redcar, TS10 4XX, UK*

This journal is © the Owner Societies 2012

Phys. Chem. Chem. Phys., 2012, **14**, 16279–16285 | 16279

Scheme 1 Spin trapping mechanism for DMPO with a free radical (R•).

this addition, known as the spin adduct, is a persistent free nitroxide radical with a sufficiently long lifetime to enable detection by conventional EPR spectroscopy (Scheme 1).[29] Because of the hyperfine coupling between the unpaired electron in the spin adduct and the ^{1}H in the beta position for the chosen spin trap, it is often possible to assign the structure of the original short-lived radicals due to changes in the ^{14}N and ^{1}H hyperfine coupling constants of the spin trap molecule.[30] In this paper we present the results of this mechanistic study.

2. Materials and methods

2.1 Chemicals

DMPO, toluene, dichloromethane, chloroform and other chemicals were purchased from *Aldrich* and used without further purification unless otherwise specified.

2.2 EPR experiments

X-band continuous wave (CW) EPR spectra were recorded at room temperature in deoxygenated cyclohexane, using a Bruker EMX spectrometer. The typical instrument parameters were: centre field 3487 G, sweep width 100 G, sweep time 55 s, time constant 10 ms, power 5 mW, modulation frequency 100 kHz, and modulation width 1 G. Quantitative spectral analysis was carried out using WinSim software.[31]

The spin trapping experiments were performed using the following procedure: 5,5-dimethyl-1-pyrroline-*N*-oxide (DMPO) (0.1 mL of 0.1 M solution in cyclohexane) was added to the substrate (0.1 mL of 2.5 molar% solution of cyclohexyl-hydroperoxide – hereafter abbreviated CHHP – in cyclohexane), in an EPR sample tube. The mixture was deoxygenated by bubbling N_2 for 1 min prior to recording the EPR spectra in order to enhance the signal intensity.[30] For the samples containing the Au/MgO catalyst, deoxygenation was carried out at room temperature, 5 min after the mixing of the catalyst with the reaction mixture.

2.3 Catalyst activity studies and product analysis

Catalytic oxidation of cyclohexane (*Alfa Aesar*, 8.5 g, HPLC grade) was carried out in a glass bench reactor using 6 mg of catalyst in 10 mL of cyclohexane. The reaction mixture was magnetically stirred at 140 °C under 3 bar O_2 for 17 hours. Samples of the reaction mixture were periodically analyzed by gas chromatography (Varian 3200) with a CP-Wax 42 column. Adipic acid was converted to its corresponding ester for quantification purposes and chlorobenzene added as internal standard.

2.4 Catalyst preparation

Au/MgO catalysts were prepared *via* impregnation of an aqueous solution (1 mL) of $HAuCl_4 \cdot 3H_2O$ (*JM*, assay 49%,) over MgO (*BDH*, 1 g), in order to obtain a gold loading of 1 wt%. The suspension was continuously stirred for 30 min. The sample was dried at 120 °C overnight and consecutively calcined at 300 °C for two hours. The same procedure was applied for the preparation at 0.1 and 0.01 wt% Au loading, adjusting accordingly the Au amount in the starting aqueous solution.

2.5 Catalyst characterization by XRPD

X-ray powder diffraction patterns (XRPD) were acquired using a X'Pert PANalytical diffractometer operating at 40 kV and 40 mA selecting the Cu-Kα radiation. Analysis of the patterns was carried out using X'Pert HighScore Plus software. In order to enhance the signal for the assignment and determination of line broadening in the Au peaks, XRPD patterns were base line corrected, and the signal-to-noise ratio was increased using a Gaussian filter. The peak identification was carried out using a second derivative algorithm to further enhance the signal. Crystallite sizes for the metal and metal oxide clusters was determined using the Scherrer equation[32] assuming spherical particle shapes and a K factor of 0.89. The line broadening was determined using a Voigt profile function,[33] convoluting the Gaussian and Lorentzian profile part of the reflection peak and the instrumental broadening for the Bragg–Brentano geometry used was estimated to be 0.06° 2θ.

2.6 Catalyst characterization by DR-UV

UV-Vis diffuse reflectance spectra were collected using a Harrick Praying Mantis cell mounted on a Varian Cary 4000 spectrophotometer. The spectra were collected from 900 to 200 nm at a scan speed of 60 nm min^{-1}. Background correction was carried out using teflon powder (Spectralon). The sample was mounted on a 3 mm diameter diffuse reflectance sampling cup.

3. Results and discussion

3.1 Catalytic tests

Au/MgO was investigated for the cyclohexane oxidation using different gold loadings in the presence and absence of radical initiators (Table 1). It is possible to observe that in the absence of radical initiators (entries 1–3), Au/MgO displays little activity; *ca.* 2% or less, when compared to autoxidation, which was in the range of *ca.* 1.1% (entry 4). However, it is evident the effect of gold on the selectivity of the reaction with enhanced cyclohexanol formation up to 50%; an effect that is lost when the amount of gold present in the catalyst is reduced. This is also reflected in variations in the amount of cyclohexyl hydroperoxide (CHHP). In fact, when the gold loading is reduced from 1 to 0.01 wt%, the selectivity to CHHP increases from 7% to *ca.* 27%, while in the absence of catalyst the selectivity to CHHP was about 57%. These data clearly indicate the influence of gold in the oxidation process, even when the metal is present in low concentrations, and including CHHP decomposition[34] and the possible quenching of some

Table 1 Conversion and selectivity of cyclohexane after 17 hours at 140 °C under 3 bar of O_2 under different reaction conditions. K = cyclohexanone, A = cyclohexanol, CHHP = cyclohexyl hydroperoxide, and AA = adipic acid

Entry	Catalyst	Au loading (wt%)	Initiator	Conversion[a] (%)	Selectivity[b] (%)					K/A ratio
					K	A	CHHP	AA	Total	
1	Au/MgO-Imp	1	—	1.9	30	51	7	0	88	0.58
2	Au/MgO-Imp	0.1	—	1.7	35	44	15	0	94	0.8
3	Au/MgO-Imp	0.01	—	1.3	28	36	27	0	91	0.78
4	Autoxidation	—	—	1.1	19	22	57	0	98	0.86
5	MgO	—	—	1.4	36	25	4	0	65	1.44
6	Au/MgO-Imp	1	AIBN	4.5	34	51	6	0	91	0.67
7	Autoxidation	—	AIBN	6.7	32	57	2	0	91	0.56
8	Au/MgO-Imp	1	TBHP	5.0	29	50	0	19	98	0.58
9	Autoxidation	—	TBHP	6.6	33	52	0	15	100	0.63

[a] We detected a closed carbon mass balance within an experimental error of 5%. [b] The missing components are carboxylic acids as ring opening products.

radicals intermediates by gold.[35,36] This relates to the catalytic decomposition of CHHP by a gold surface, which would drive the selectivity towards cyclohexanol. In fact, if only autoxidation was operative, an increase in conversion would always be accompanied by a loss of selectivity to the alcohol.[37] This is due to the fact that when autoxidation is operating, it always leads to the ketone (see Section 3.3).

However, because the conversion values are just above those obtained by autoxidation, these data suggest that the reaction still proceeds *via* a radical chain mechanism. A control experiment using MgO in the absence of gold (entry 5) showed that the conversion is higher than the one observed for autoxidation, but lower than that observed for the gold containing catalyst, where the selectivity is shifted to the ketone.

In view of this, the effect of initiators such as azo-bis-isobutyronitrile (AIBN) and *tert*-butylhydroperoxy radical (TBHP) were evaluated (Table 1). When AIBN was used (entries 6 and 7), the activity of Au/MgO catalyst increased to *ca.* 4% and with selectivity values quite similar to those obtained for the catalyst in absence of initiators (entry 1). However, despite this apparent increase in conversion, this is less than the value obtained in the presence of AIBN only (*ca.* 7%). This is consistent with the role of Au as an inhibitor for the reaction. In contrast, if TBHP was used (entries 8 and 9), the activity of Au/MgO increased, (up to *ca.* 5%) but, also in this case, it was lower than that for the reaction carried out in presence of TBHP only (*ca.* 6.6%). Moreover, the selectivity control to cyclohexanol and cyclohexanone was limited, and a significant amount of adipic acid was detected, an effect that should be considered a direct consequence of the large amount of peroxides in solution.[38]

3.2 Nature of the catalyst

The catalyst was obtained by impregnating an aqueous solution of $HAuCl_4$ into MgO as support. In view of this preparation procedure, and the well known properties of MgO, the final material is a mixture of MgO and $Mg(OH)_2$. This was confirmed by XRPD (Fig. 1) where the following phases were identified: MgO (periclase),[39] $Mg(OH)_2$ (brucite),[40] with traces amounts of $MgCO_3$ (magnesite).[41] However, this does not affect our results and this material is referred to hereafter as Au/MgO.
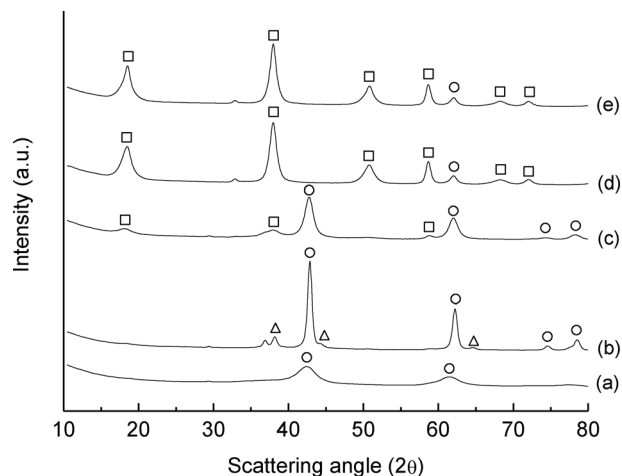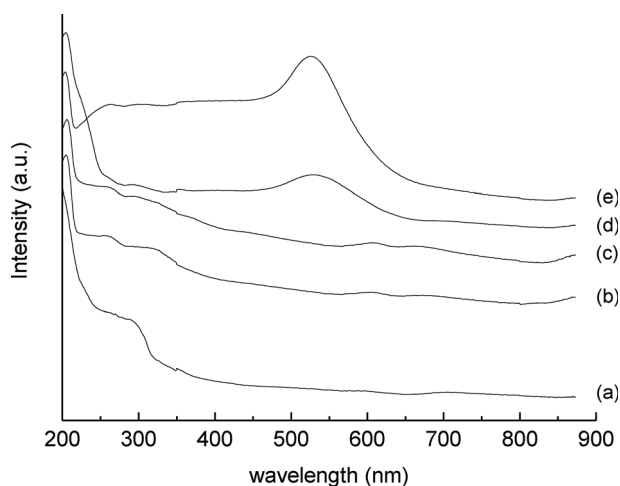

Fig. 1 XRPD patterns of: (a) MgO starting material, (b) Au/MgO catalyst 1 wt%, (c) Au/MgO catalyst 0.1 wt%, (d) Au/MgO catalyst 0.01 wt% and (e) MgO support impregnated with water. The symbols used indicate: (○) MgO – periclase (□) $Mg(OH)_2$ – brucite, and (△) Au.

From the XRPD pattern it was also possible to estimate the particle size of gold, using the Au(111) reflection at 38.2° 2θ.[42] These were estimated to be *ca.* 17 and 8 nm for the materials containing 1 and 0.1 wt% Au respectively. In contrast, no gold reflection for the 0.01 wt% Au sample was detected, indicating a particle size below the detection limit of the XRD method, which is *ca.* 4 nm. Gold nanoparticles were also well identified by means of plasmon resonance[43] *via* diffuse reflectance UV-Vis spectroscopy (Fig. 2), and the band intensity of the spectra is consistent with the particles size estimation obtained by XRPD; *i.e.*, with gold particles less than 4 nm diameter for the 0.01 wt% Au sample.

A detailed analysis of the diffuse reflectance spectra shows that MgO, even for the untreated sample, presents absorption bands in the UV range at *ca.* 210 and 280–300 nm. While MgO is commonly regarded as a white standard for DR-UV in the visible region,[44] absorption bands at 213 nm and 282 nm are associated with the excitation of four-fold and three-fold coordinated surface O^{2-} anions at edge and corner positions of MgO crystals respectively.[45,46] This is a consequence of the use of a commercial purity grade MgO as catalyst support, rather than the use of an optically purity grade MgO.

Fig. 2 Diffuse reflectance UV-Vis spectra of: (a) MgO starting material, (b) MgO support impregnated with water, (c) Au/MgO catalyst 0.01 wt%, (d) Au/MgO catalyst 0.1 wt% and (e) Au/MgO catalyst 1 wt%.

3.3 Free radical chain mechanism

In order to rationalize the results described above on the behaviour of Au/MgO catalyst, it is important to consider the accepted free radical chain reaction mechanism in the autoxidation case, and the different decomposition pathways for AIBN and TBHP. The commonly accepted radical chain pathway in the formation of cyclohexanol and cyclohexanone is reported in Scheme 2 (eqn (1)–(7)).[47,48]

The first step of the oxidation is the initiation, which involves activation of the C–H bond *via* abstraction of an H atom. This can occur by a number of events, including: (i) cleavage by an unsaturated metal centre,[49] (ii) H abstraction by a peroxide species (either peroxyl or alkoxy radicals present in solution),[28] or (iii) H abstraction by a superoxide species (O_2^-) bound to metal centres or metal oxides.[50] For each of these processes this results in the formation of a carbon centred parent radical ($C_6H_{11}^\bullet$). It is well known that carbon-centred radicals are extremely reactive[51] and they immediately react with O_2 to give peroxyl radicals, in our case cyclohexyl peroxyl radical (C_6H_{11}–$OO^\bullet$) according to (eqn (2)). In principle, the oxygen
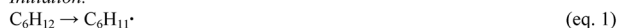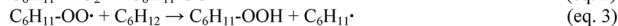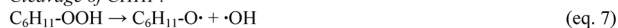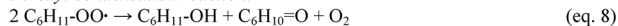
incorporated into the products can originate from oxygen dissolved in solution or from adsorbed oxygen species on the metal oxide surface.[52] C_6H_{11}–$OO^\bullet$ can react further with cyclohexane to give cyclohexyl hydroperoxide (CHHP) and another $C_6H_{11}^\bullet$ radical, thus ensuring propagation of the reaction (eqn (3)). It should be stressed that, in this scheme C_6H_{11}–$OO^\bullet$ is the main radical chain carrier, with CHHP reacting in a sequence that finally yields cyclohexanone (eqn (4) and (5)).

In contrast, cyclohexanol can be obtained by hydrogenation of cyclohexyl alkoxy radical C_6H_{11}–$O^\bullet$ (eqn (6)), cleavage of CHHP (eqn (7)) or *via* recombination of two peroxyl radicals (eqn (8)).[53] In principle, cyclohexanol can originate from insertion of lattice oxygen from the metal oxide to the $C_6H_{11}^\bullet$ parent radical adsorbed over the catalyst surface.[54] However, when MgO only was tested, no activity was detected which therefore rules out this latter possible route, and this is also not related to the purity level of MgO.
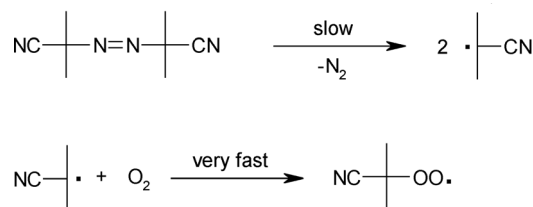
From this model, it is evident that the ketone is always obtained (eqn (5) and (8)) if autoxidation is operating. Therefore selectivity control, if any, can occur only in the decomposition step of CHHP (eqn (7)). More recently, solvent-cage models have also been proposed for the autoxidation pathways,[55] to explain the alcohol and ketone formation.
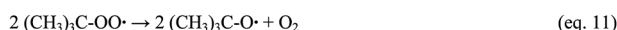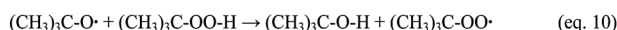
3.4 Radical initiators

In this context, radical initiators were used to promote the oxidation reaction. However, it is necessary to emphasise that AIBN and TBHP, despite both being radical initiators, operate through a different decomposition pathway and this can help to explain the differences in reactivity observed in the present study. AIBN is thermally decomposed to two cyanopropyl radicals and N_2 (Scheme 3).[51] Carbon centred radicals are extremely reactive and they can instigate H abstraction, or they can react further with the oxygen present in the reaction media to form peroxy radicals. The new cyanopropyl peroxy radical can also act as a H abstractor, and therefore initiate the reaction acting on eqn (1).

In contrast TBHP can undergo homolytic cleavage of the O–O bond and from this to peroxyl condensation *via* the set of equations ((9)–(11)) reported in Scheme 4.[56]

Considering the mechanisms of action for these initiators and the results obtained in the current case (*i.e.*, an enhanced oxidation when initiators are used, but a decrease when

Initiation:
$$C_6H_{12} \rightarrow C_6H_{11}^\bullet \qquad \text{(eq. 1)}$$

Propagation:
$$C_6H_{11}^\bullet + O_2 \rightarrow C_6H_{11}\text{-}OO^\bullet \qquad \text{(eq. 2)}$$
$$C_6H_{11}\text{-}OO^\bullet + C_6H_{12} \rightarrow C_6H_{11}\text{-}OOH + C_6H_{11}^\bullet \qquad \text{(eq. 3)}$$

Cyclohexanone formation:
$$C_6H_{11}\text{-}OO^\bullet + C_6H_{11}OOH \rightarrow C_6H_{11}OOH + C_6H_{10}(^\bullet)OOH \qquad \text{(eq. 4)}$$
$$C_6H_{10}(^\bullet)OOH \rightarrow C_6H_{10}\text{=}O + {}^\bullet OH \qquad \text{(eq. 5)}$$

Cyclohexanol formation:
$$C_6H_{11}\text{-}O^\bullet + C_6H_{12} \rightarrow C_6H_{11}\text{-}OH + C_6H_{11}^\bullet \qquad \text{(eq. 6)}$$

Cleavage of CHHP:
$$C_6H_{11}\text{-}OOH \rightarrow C_6H_{11}\text{-}O^\bullet + {}^\bullet OH \qquad \text{(eq. 7)}$$

Peroxyl condensation reaction:
$$2\ C_6H_{11}\text{-}OO^\bullet \rightarrow C_6H_{11}\text{-}OH + C_6H_{10}\text{=}O + O_2 \qquad \text{(eq. 8)}$$

Scheme 2 Radical chain pathway in the formation of cyclohexanol and cyclohexanone during the oxidation of cyclohexane.

Scheme 3 AIBN decomposition pathway.

$$(CH_3)_3C\text{-}OO\text{-}H \rightarrow (CH_3)_3C\text{-}O^\bullet + {}^\bullet OH \qquad \text{(eq. 9)}$$
$$(CH_3)_3C\text{-}O^\bullet + (CH_3)_3C\text{-}OO\text{-}H \rightarrow (CH_3)_3C\text{-}O\text{-}H + (CH_3)_3C\text{-}OO^\bullet \qquad \text{(eq. 10)}$$
$$2\ (CH_3)_3C\text{-}OO^\bullet \rightarrow 2\ (CH_3)_3C\text{-}O^\bullet + O_2 \qquad \text{(eq. 11)}$$

Scheme 4 TBHP decomposition pathway.

16282 | *Phys. Chem. Chem. Phys.*, 2012, **14**, 16279–16285

This journal is © the Owner Societies 2012

combined with Au/MgO) it would be possible to conclude that Au/MgO can actually quench some of the radicals generated by the initiators, such as cyanopropyl radicals,[57,58] but at the same time acting as a promoter for the O–O cleavage in the TBHP decomposition;[34–36] this could also explain the enhanced selectivity to cyclohexanol. It is possible that quenching comes at least in part from the support, with the activation role from the metal nanoparticle counterpart. Many metal oxides, such as MgO, present neutral oxygen vacancies[59,60] that could possibly aid in the localisation of peroxyl species, and so partially inhibit the reaction when initiators are used. A similar quenching effect was observed for ZnO in the aldehyde oxidation by Au/ZnO catalysts.[61] In fact, regardless of the insulator properties of MgO, compared to the semi-conducting properties of ZnO which may increase the tendency to radical quenching, the presence of defects in or on the MgO crystals may facilitate radical trapping and stabilisation.[62] This effect has been experimentally observed for methyl radicals in gas phase.[63]

3.5 EPR spin trapping experiments

In order to explain the enhanced selectivity to the alcohol when Au is used, spin trapping was carried out in presence of CHHP using 5,5-dimethyl-1-pyrroline-N-oxide (DMPO) as the spin trap. CHHP was chosen for two reasons: it is a peroxide involved in the cyclohexane oxidation, and it can be prepared free of water, which could interfere in the determinations.

When the reaction was carried out at room temperature in the presence of DMPO as spin trap, CW EPR spectra were acquired in the presence (Fig. 3) and absence (Fig. 4) of Au/MgO. Simulation of the spectrum and comparison with literature values allowed the identification of all the radical intermediates which are expected in the autoxidation pathway of cyclohexane to cyclohexanone and cyclohexanol. In particular these species include: di-tert-butyl-nitroxide derivative,[64] a DMPO–O–C_6H_{11}[65] and a DMPO–OOC_6H_{11} spin adduct,[66]
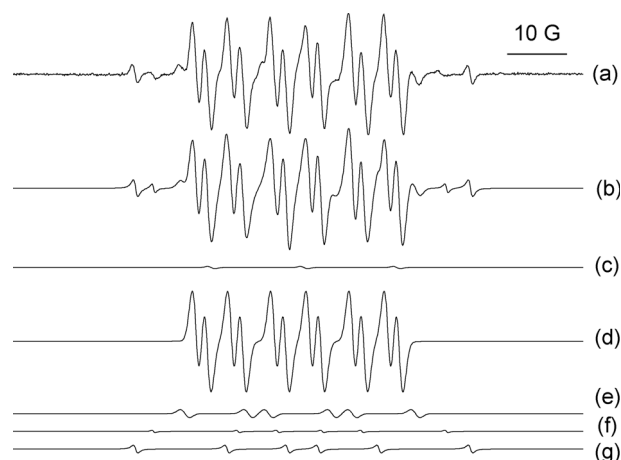
Fig. 3 Deconvoluted EPR spectra of DMPO spin adducts obtained during the decomposition of CHHP in cyclohexane in the presence of Au/MgO: (a) experimental spectrum and (b) simulated spectrum; (c) di-tert-butyl-nitroxide derivative, (d) DMPO–O–C_6H_{11} spin adduct, (e) a DMPO–OO–C_6H_{11} adduct, (f) DMPO–C_6H_{11} carbon centred adduct, and (g) carbon centred adduct, which is possibly a DMPO–C(OH)R_2 species.
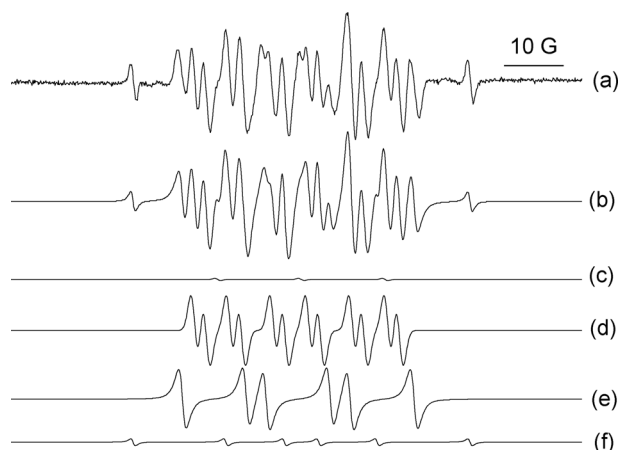
Fig. 4 Deconvoluted EPR spectra of the DMPO spin adducts obtained during cyclohexane autoxidation at room temperature in the presence of CHHP: (a) experimental spectrum and (b) simulated spectrum; (c) di-tert-butyl-nitroxide derivative, (d) DMPO–O–C_6H_{11} spin adduct, (e) DMPO–OO–C_6H_{11} adduct, and (f) carbon centred adduct which is possibly a DMPO–C(OH)R_2 species.

Table 2 Hyperfine splitting constants (in Gauss) for the DMPO spin adducts, obtained during the decomposition of CHHP in cyclohexane, in presence and absence of Au/MgO catalyst. The values in bracket are in absence of catalyst, and n.d. = not detected

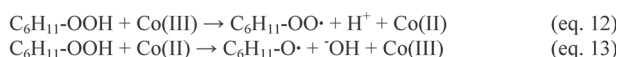| Radical	a_N/G	$a_{H(\beta)}$/G	$a_{H(\gamma)}$/G
tert-Butyl nitroxide derivative	14.2 (14.2)	—	—
C_6H_{11}–O•	13.4 (13.4)	6.00 (6.00)	1.80 (1.90)
C_6H_{11}–OO•	14.3 (14.2)	10.8 (10.8)	
C_6H_{11}•	14.3 (n.d.)	21.2 (n.d.)	
$R_2(OH)C$•	15.6 (15.8)	25.9 (25.7)	

a DMPO–C_6H_{11} carbon-centred adduct characteristic of the parent radical C_6H_{11}•[67] and a carbon centred adduct which is possibly a DMPO–C(OH)R_2 species.[68] The spin Hamiltonian parameters of these spin adducts are reported in Table 2.

It should be noted that the spin trapping technique only allows for semi-quantitative determination of the adducts detected. This is a consequence of the life-time of the spin adduct, the nature of the solvent, the temperature and the efficiency of the capture reaction which is different for each radical.[28,30] With these limitation in mind, the simulation revealed the following semi-quantitative values: di-tert-butyl-nitroxide derivative (2%); DMPO–O–C_6H_{11} (81%); DMPO–OO–C_6H_{11} (8%); DMPO–C_6H_{11} (4%); and possible DMPO–C(OH)R_2 adduct (5%).

When the same experiment was carried out in the absence of Au/MgO, to assess the CHHP decomposition via the autoxidation pathway, the following species were obtained (Fig. 4): di-tert-butyl-nitroxide derivative, DMPO–O–C_6H_{11} and DMPO–OO–C_6H_{11} spin adducts and the possible DMPO–C(OH)R_2 adduct. The hyperfine splitting constants of these spin adducts are reported in Table 2. These species were quantified as follow: di-tert-butyl-nitroxide derivative (2%); DMPO–O–C_6H_{11} (50%); DMPO–OO–C_6H_{11} (43%); and DMPO–C(OH)R_2 (5%).

The species trapped in the presence and absence of Au/MgO are basically the same in both sets of experiments, but the

$$C_6H_{11}\text{-}OOH + Co(III) \rightarrow C_6H_{11}\text{-}OO\bullet + H^+ + Co(II) \qquad (eq.\ 12)$$
$$C_6H_{11}\text{-}OOH + Co(II) \rightarrow C_6H_{11}\text{-}O\bullet + {}^-OH + Co(III) \qquad (eq.\ 13)$$

Net equation:

$$2C_6H_{11}\text{-}OOH \rightarrow C_6H_{11}\text{-}OO\bullet + C_6H_{11}\text{-}O\bullet + H_2O \qquad (eq.\ 14)$$

Scheme 5 Haber–Weiss cycle for the oxidation of cyclohexane mediated by Co(III).

parent radical is not detected in the autoxidation case. In contrast, the most remarkable difference between the two sets is an increased quantity of alkoxy (C_6H_{11}–$O^\bullet$) species, from 50% to 80% when gold is used. This indicates that Au/MgO is capable of enhancing alcohol formation by cleavage of the O–O bond of CHHP.

However, as the spin trapping technique is prone to artifacts, control tests were necessary and we carefully carried out. In fact, spin adducts can be formed not just by the radical addition to a spin trap, but also by nucleophilic addition followed by oxidation of the spin adduct[69,70] or by oxidation of the spin trap followed by nucleophilic addition, in our case by species such as ^-OH. Control tests in the presence of Au/MgO and the spin trap, but in the absence of substrate, did not reveal any trace of the DMPOX oxidation product.[71] Moreover, the trace amount of di-*tert*-butyl-nitroxide derivative should be considered ubiquitous in these types of experiments and can be discounted.[28,61]

On the other hand, no DMPO–OH adduct was detected in the tests we carried out. If homolytic cleavage of a substrate is considered, it is not unprecedented, by using spin trapping, to detect just one of the two expected partners (in our case RO$^\bullet$). This could be due to a failure of the spin trap molecule to capture the $^\bullet OH$ species under the reaction conditions used, or by termination of $^\bullet OH$ on the metal surface. In addition, it is known that $^\bullet OH$ is among the most reactive known radical species,[72] and therefore difficult to trap.

This still does not preclude a redox cycle mediated by the metal centre. At present, this has been accredited in the case of oxidation by means of Co(III) salts in agreement with the Haber–Weiss cycle,[73] (Scheme 5, eqn (12)–(14)).

No adduct from nucleophilic attack and oxidation was detected when Au was present. Moreover, systems like those in eqn (12)–(14) have a K/A ratio in the range of 1.5,[2,21] while in our case the K/A ratio is in the range of 0.6 with clear selectivity to the alcohol, therefore supporting the conclusion that gold has to operate a homolytic cleavage of CHHP in agreement with eqn (7).

3.6 Effect of CBrCl$_3$ as radical scavenger

In view of the data reported so far, supported gold nanoparticles appear to be capable of accelerating the reaction rate (although to a minor extent) but within the autoxidation pathway, *i.e.*, without inducing alternative reaction mechanisms or intermediates from those that would be expected from the free radical chain mechanism. In order to test this hypothesis, a reaction in the presence of CBrCl$_3$ was carried out. CBrCl$_3$ can act as radical scavenger by cleavage of the C–Br bond by carbon centred radicals.[74] Therefore, CBrCl$_3$ is capable of reacting with the parent $C_6H_{11}^\bullet$ radical to yield to C_6H_{11}–Br and thus quench the reaction.
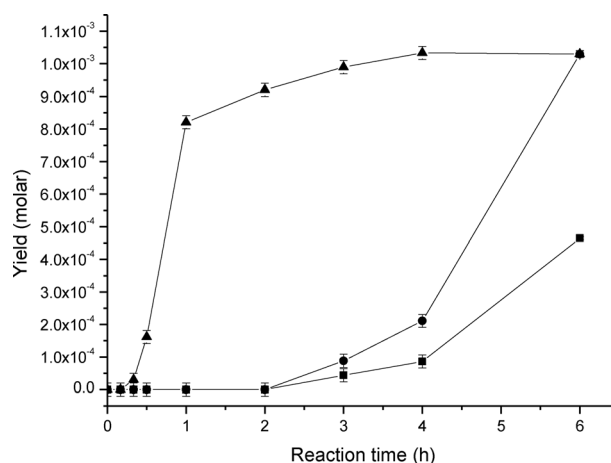
Fig. 5 Product evolution in the liquid phase oxidation of cyclohexane over Au/MgO in presence of CBrCl$_3$ as radical scavenger at 140 °C under 3 bar of O$_2$: (▲) bromocyclohexane, (●) cyclohexanol and (■) cyclohexanone.

When CBrCl$_3$ was used (Fig. 5) the reaction was completely inhibited at the initial stage (first 2 hours). Then as long as CBrCl$_3$ was consumed in the reaction media, with consequent C_6H_{11}–Br formation which is detected after *ca.* 30 min, product formation is observed. In particular, when all CBrCl$_3$ was consumed (after 2 hours), the oxidation reaction newly started as in the absence of inhibitor, thus demonstrating that Au/MgO promotes the decomposition of CHHP but within a free radical-chain reaction mechanism.

4. Conclusions

The current literature on the use of Au based catalysts in cyclohexane oxidation describes the role of Au to be that of either a true catalyst or a mere promoter for the reaction. The present study shows a situation which should be considered as intermediate within these two extremes. In fact, Au is capable of accelerating the reaction, without the need for initiators, and so it is by definition a catalyst for the cyclohexane oxidation, but this acceleration occurs by increasing the concentration of species (through C_6H_{11}–OOH or C_5H_{11}–OO$^\bullet$) which are chain carriers in the radical pathway of the reaction and therefore promote catalytic autoxidation processes *via* a radical-chain mechanism. These findings can shed light on the use of gold catalysts for alkane oxidations showing that selectivity control is possible but with a limited effect on the conversion of the reaction.

Acknowledgements

Notes and references

1 J. G. Speight, *Chemical and Process Design Handbook*, McGraw-Hill, New York, 2002, p 2.185.
2 A. Ramanathan, M. S. Hamdy, R. Parton, T. Maschmeyer, J. C. Jansen and U. Hanefeld, *Appl. Catal., A*, 2009, **355**, 78–82.
3 H. C. Shen and H. S. Weng, *Ind. Eng. Chem. Res.*, 1988, **27**, 2254–2260.

4 A. F. Masters, J. K. Beattie and A. L. Roa, *Catal. Lett.*, 2001, **75**, 159–162.

5 V. Govindan and A. K. Suresh, *Ind. Eng. Chem. Res.*, 2007, **46**, 6891–6898.

6 C. Hettige, K. R. R. Mahanama and D. P. Dissanayake, *Chemosphere*, 2001, **43**, 1079–1083.

7 M. Conte and V. Chechik, *Chem. Commun.*, 2010, **46**, 3991–3993.

8 U. Schuchardt, D. Cardoso, R. Sercheli, R. Pereira, R. S. de Cruz, M. C. Guerreiro, D. Mandelli, E. V. Spinace and E. L. Fires, *Appl. Catal., A*, 2001, **211**, 1–17.

9 G. P. Chiusoli and P. M. Maitlis, *Metal-catalysis in Industrial Organic Processes*, RSC Publising, Cambridge, 2008, p 29.

10 L. X. Xu, C. H. He, M. Q. Zhu and S. Fang, *Catal. Lett.*, 2007, **114**, 202–205.

11 G. M. Lu, D. Ji, G. Qian, Y. X. Qi, X. L. Wang and J. S. Suo, *Appl. Catal., A*, 2005, **280**, 175–180.

12 K. K. Zhu, J. C. Hu and R. Richards, *Catal. Lett.*, 2005, **100**, 195–199.

13 L. Li, C. Jin, X. C. Wang, W. J. Ji, Y. Pan, T. van der Knaap, R. van der Stoel and C. T. Au, *Catal. Lett.*, 2009, **129**, 303–311.

14 Y.-J. Xu, P. Landon, D. Enache, A. Carley, M. Roberts and G. Hutchings, *Catal. Lett.*, 2005, **101**, 175–179.

15 C. Della Pina, E. Falletta, L. Prati and M. Rossi, *Chem. Soc. Rev.*, 2008, **37**, 2077–2095.

16 A. S. K. Hashmi and G. J. Hutchings, *Angew. Chem., Int. Ed.*, 2006, **45**, 7896–7936.

17 M. D. Hughes, Y.-J. Xu, P. Jenkins, P. McMorn, P. Landon, D. I. Enache, A. F. Carley, G. A. Attard, G. J. Hutchings, F. King, E. H. Stitt, P. Johnston, K. Griffin and C. J. Kiely, *Nature*, 2005, **437**, 1132–1135.

18 C. Della Pina, E. Falletta and M. Rossi, *Chem. Soc. Rev.*, 2012, **41**, 350–369.

19 L. X. Xu, C. H. He, M. Q. Zhu, K. J. Wu and Y. L. Lai, *Catal. Lett.*, 2007, **118**, 248–253.

20 L. X. Xu, C. H. He, M. Q. Zhu, K. J. Wu and Y. L. Lai, *Catal. Commun.*, 2008, **9**, 816–820.

21 P. C. Hereijgers and B. M. Weckhuysen, *J. Catal.*, 2010, **270**, 16–25.

22 Y. Liu, H. Tsunoyama, T. Akita, S. Xie and T. Tsukuda, *ACS Catal.*, 2011, **1**, 2–6.

23 G. L. Brett, Q. He, C. Hammond, P. J. Miedziak, N. Dimitratos, M. Sankar, A. A. Herzing, M. Conte, J. A. Lopez-Sanchez, C. J. Kiely, D. W. Knight, S. H. Taylor and G. J. Hutchings, *Angew. Chem., Int. Ed.*, 2011, **50**, 10136–10139.

24 J. Guzman and B. C. Gates, *J. Am. Chem. Soc.*, 2004, **126**, 2672–2673.

25 M. S. Chen and D. W. Goodman, *Catal. Today*, 2006, **111**, 22–33.

26 P. Ionita, B. C. Gilbert and V. Chechik, *Angew. Chem., Int. Ed.*, 2005, **44**, 3720–3722.

27 A. Burt, M. Emery, J. Maher and B. Mile, *Magn. Reson. Chem.*, 2001, **39**, 85–88.

28 M. Conte, K. Wilson and V. Chechik, *Org. Biomol. Chem.*, 2009, **7**, 1361–1367.

29 M. Conte, H. Miyamura, S. Kobayashi and V. Chechik, *J. Am. Chem. Soc.*, 2009, **131**, 7189–7196.

30 P. Ionita, M. Conte, B. C. Gilbert and V. Chechik, *Org. Biomol. Chem.*, 2007, **5**, 3504–3509.

31 Simulations were carried out using WinSim software: http://www.niehs.nih.gov/research/resources/software/tox-pharm/tools/index.cfm.

32 B. D. Cullity and S. R. Stock, *Elements of X-Ray Diffraction*, Prentice-Hall Inc., Upper Saddle River, 3rd edn, 2001, p. 161.

33 J. I. Langford, *J. Appl. Crystallogr.*, 1978, **11**, 10–14.

34 J. R. Sanderson, M. A. Mueller and Y.-H. E. Sheu, *US Patent*, 5401889, 1995.

35 J. D. Druliner, K. Kourtakis and L. E. Manzer, *International Patent*, WO 98/34894, 1998.

36 N. Herron, S. Schwarz and J. D. Druliner, *International Patent*, WO 02/16296, 2002.

37 N. Turrà, A. B. Acuņa, B. Schimmöller, B. Mayr-Schmölzer, P. Mania and I. Hermans, *Top. Catal.*, 2011, **54**, 737–745.

38 K. Sato, M. Aoki and R. Noyori, *Science*, 1998, **281**, 1646–1647.

39 A. Kern, R. Doetzer and W. Eysel, ICDD Grant-in-Aid, 1993, in International Centre for Diffraction Data, Powder Diffraction File, Entry 45-946, 1996.

40 US Natl. Bur. Stand., 1956, in International Centre for Diffraction Data, Powder Diffraction File, Entry 7-239, 1996.

41 US Natl. Bur. Stand., 1957, in International Centre for Diffraction Data, Powder Diffraction File, Entry 8-479, 1996.

42 US Natl. Bur. Stand., 1953, in International Centre for Diffraction Data, Powder Diffraction File, Entry 4-784, 1996.

43 W. W. Weare, S. M. Reed, M. G. Warner and J. E. Hutchison, *J. Am. Chem. Soc.*, 2000, **122**, 12890–12891.

44 R. G. J. Strens and B. J. Wood, *Mineral. Mag.*, 1979, **43**, 347–354.

45 F. Gu, C. Li, H. Cao, W. Shao, Y. Hu, J. Chen and A. Chen, *J. Alloys. Compd.*, 2008, **453**, 361–365.

46 S. Stankic, M. Müller, O. Diwald, M. Sterrer, E. Knözinger and J. Bernardi, *Angew. Chem., Int. Ed.*, 2005, **44**, 4917–4920.

47 C. A. Tolman, J. D. Druliner, M. J. Nappa and N. Herron, *Activation and Functionalization of Alkanes*, Wiley, New York, 1989, p. 303.

48 L. Vereecken, T. L. Nguyen, I. Hermans and J. Peeters, *Chem. Phys. Lett.*, 2004, **393**, 432–436.

49 S. Bhaduri and D. Mukesh, *Homogeneous Catalysis: Mechanisms and Industrial Applications*, John Wiley & Sons Inc., New York, 2000, p. 179.

50 D. Mandon, H. Jaafar and A. Thibon, *New J. Chem.*, 2011, **35**, 1986–2000.

51 M. Conte, Y. Ma, C. Loyns, P. Price, D. Rippon and V. Chechik, *Org. Biomol. Chem.*, 2009, **7**, 2685–2687.

52 R. Schlögl, A. Knop-Gericke, M. Hävecker, U. Wild, D. Frickel, T. Ressler, R. E. Jentoft, J. Wienold, G. Mestl, A. Blume, O. Timpe and Y. Uchida, *Top. Catal.*, 2001, **15**, 219–228.

53 I. Hermans, P. Jacobs and J. Peeters, *Chem.–Eur. J.*, 2006, **13**, 754–761.

54 B. Modén, B.-Z. Zhan, J. Dakka, J. G. Santiesteban and E. Iglesia, *J. Catal.*, 2006, **239**, 390–401.

55 I. Hermans, T. L. Nguyen, P. A. Jacobs and J. Peeters, *ChemPhysChem*, 2005, **6**, 637–645.

56 C. Walling and L. Heaton, *J. Am. Chem. Soc.*, 1965, **87**, 38–47.

57 M. Álvaro, C. Aprile, A. Corma, B. Ferrer and H. García, *J. Catal.*, 2007, **245**, 249–252.

58 K. L. Mcgilvray, M. R. Decan, D. Wang and J. C. Scaiano, *J. Am. Chem. Soc.*, 2006, **128**, 15980–15981.

59 L. Dall'Acqua, I. Nova, L. Lietti, G. Ramis, G. Buscac and E. Giamello, *Phys. Chem. Chem. Phys.*, 2000, **2**, 4991–4998.

60 G. Mestl, N. F. D. Verbruggen, E. Bosch and H. Knözinger, *Langmuir*, 1996, **12**, 2961–2968.

61 M. Conte, H. Miyamura, S. Kobayashi and V. Chechik, *Chem. Commun.*, 2010, **46**, 145–147.

62 D. Ricci, G. Pacchioni, P. V. Sushko and A. L. Shluger, *J. Chem. Phys.*, 2002, **117**, 2844–2851.

63 D. J. Driscoll, W. Martyr, J.-X. Wang and J. H. Lunsford, *J. Am. Chem. Soc.*, 1985, **107**, 58–63.

64 M. Novak and B. A. Brodeur, *J. Org. Chem.*, 1984, **49**, 1142–1144.

65 S. L. Baum, I. G. M. Anderson, R. R. Baker, D. M. Murphy and C. C. Rowlands, *Anal. Chim. Acta*, 2003, **481**, 1–13.

66 M. J. Davies and T. F. Slater, *Biochem. J.*, 1986, **240**, 789–795.

67 E. G. Janzen, C. A. Evans and J.-P. Liu, *J. Magn. Reson.*, 1973, **9**, 513–516.

68 M. Conte, K. Wilson and V. Chechik, *Rev. Sci. Instrum.*, 2010, **81**, 104102.

69 P. Ionita, B. C. Gilbert and A. C. Whitwood, *J. Chem. Soc., Perkin Trans. 2*, 2000, 2436–2440.

70 P. Ionita, B. C. Gilbert and A. C. Whitwood, *Lett. Org. Chem.*, 2004, **1**, 70–74.

71 V. Chechik, M. Conte, T. Dransfield, M. North and M. Omedes-Pujol, *Chem. Commun.*, 2010, **46**, 3372–3374.

72 W.-F. Wang, M. N. Schuchmann, H.-P. Schuchmann, W. Knolle, J. von Sonntag and C. von Sonntag, *J. Am. Chem. Soc.*, 1999, **121**, 238–245.

73 R. P. Houghton and C. R. Rice, *Polyhedron*, 1996, **15**, 1893–1897.

74 S. V. Dvinskikh, A. V. Yurkovskaya and H.-M. Vieth, *J. Phys. Chem.*, 1996, **100**, 8125–8130.